Electronic Supplementary Material (ESI) for Physical Chemistry Chemical Physics.
This journal is © the Owner Societies 2014

Supporting Information

Quantification of Protein-Materials Interaction by Soft Colloid Probe Spectroscopy

Steve Martin, Hanqing Wang, Laura Hartmann, Tilo Pompe, Stephan Schmidt.[‡]*

S1 Polyacrylic acid (PAA) SCP preparation

Materials

Acrylic acid and ammonium persulfate (APS) were purchased from Sigma Aldrich. Bis (N, N'-Methylene-bis-acrylamide) (MBAm) was purchased from Alfa Aesar. High viscosity (220-260 mm^2/s) paraffin oil was purchased from Carl Roth. Toluene and isopropanol were purchased from VWR. Polyglycerol Polyricinoleate (PGPR) was a gift from Danisco DuPont. Cetyl PEG/PPG-10/1 Dimethicone (ABIL EM 90) was a gift from Evonik.

Synthesis of the microparticles

Acrylic acid, MBAm and APS were dissolved in 10 mL MilliQ water at a concentration of 13.04 wt%, 0.26 wt% and 0.13 wt%, respectively. To 97 g high viscosity paraffin oil, PGPR and ABIL EM 90 as emulsifiers were added at a concentration of 2 wt% and 1 wt% , respectively . Both solutions were mixed at a ratio of 1:6 by a Carl Roth IKA mini shaker (30 s, 2500 rpm) (Carl Roth, Germany) to form a total volume of 3.5 mL emulsion. The emulsion was heated at 80 °C for 3 h using a Heraeus Vacutherm oven (Thermo Scientific, Germany) to initiate polymerization. The resulting microparticles were isolated by centrifugation at 5000 rpm for 10 min and washed 3 times with toluene/water (1:1), 3 times with isopropanol and 3 times with water to remove emulsifiers, paraffin oil and other impurities.

Remarks:

The name "Cetyl PEG/PPG-10/1 Dimethicone (ABIL EM 90)" is INCI (International Nomenclature of Cosmetic Ingredients) name.

S2 SCP protein functionalization

Materials

Sulfo *N*-Hydroxysuccinimide (sulfo-NHS), sodium phosphate, phosphate buffer saline (PBS) and 2-(*N*-morpholino)ethanesulfonic acid buffer (MES-buffer) were purchased from Sigma Aldrich.

1-Ethyl-3-(3-dimethylaminopropyl)carbodiimide (EDC) was purchased from Merck KGaA. Fibronectin was isolated from human plasma.

Protein coupling

The microparticles were transferred in 0.1M MES buffer (pH 5) by threefold centrifugation at 5000 rpm for 5 min and substitution of the remaining supernatant. Sulfo-NHS and EDC were dissolved in 1 mL 0.1M MES buffer (pH 5) at a concentration of 0.1 M, respectively. To activate the acrylic acids of the microparticles, the sulfo-NHS-EDC-solution was added for 1hrs at room temperature. The activated microparticles were washed 3 times in 0.1M MES buffer (pH 5) and afterwards added to a protein solution in 0.1 M phosphate buffer (pH 8) with a protein concentration of 0.2 mg/ml FN, respectively. The coupling process was in progress over night at 4°C while rocking. The functionalized microparticles were washed 2 times with PBS and stored in PBS with 0.1wt% sodium azide.

S3 Imaging the protein layer via confocal laser scanning microscopy

Protein functionalized SCPs were functionalized in Rhodamin-FITC (0.1 mg/ml, 100 mM $NaHCO_3$) and imaged on a Zeiss LSM 700 in order to visualize protein localization. FN functionalized SCP show a strong and homogenous localization of fluorescence at the SCP surface indicating a dense and homogenous coverage of SCP by FN.

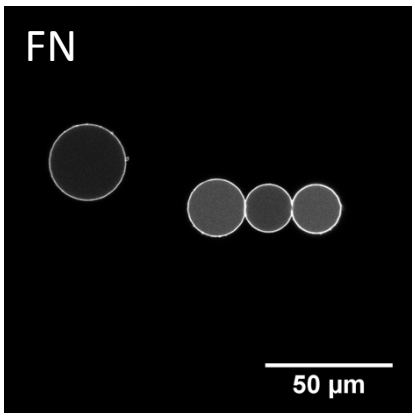

S4 Estimation of protein surface density and adhesion energy per mole

FN (hydrodynamic radius 11.5 nm) is larger than the average mesh size of the PAA matrix[1] (5.7 nm) and should preferably bind at the surface of the SCPs as proven in S3.[1] Therefore we could assume a dense packing on the SCP surface. If we assume an average spacing of the proteins on the SCP surface of 23 nm for FN (twice the hydrodynamic radius) we arrive at a monolayer density of 3.1×10^{-9} mol/m^2. With the protein density and the surface energy per area at hand we can calculate the adhesion energies per mole of proteins, see table below.

MA-copolymer	FN adhesion energy (kJ/mol)
PEMA	8
PPMA	17
PSMA	30
POMA	51

S5 Determination of the SCPs elastic modulus

Force spectroscopy with a NanoWizard 3 AFM system was performed to determine the elastic modulus of the microparticles. Therefore a polystyrene bead with a diameter of 7.311 µm was glued with an epoxy glue onto a tipless, non-coated cantilever (spring constant 0.32 N/m; NanoAndMore GmbH). Several force curves were recorded from different particles and analyzed with the novel contact model developed by Glaubitz et al. [2]. The model considers deformation of

[1] The mesh width ξ of the polymer gel can be estimated according to $\xi = \left(\frac{E}{2kT(1+\upsilon)} \right)^{-1/3}$. With an elastic modulus E = 66.5 KPa, a Poisson ratio v = 0.5, a temperature T = 293 K and the Boltzmann constant k we arrive at 5.7 nm.

the object at two sites: the indentation site of the AFM probe and at the contact with the solid support. The respective deformation (δ) –force (F) dependence reads:

$$\delta(F) = \left(\frac{3F}{4E}\cdot\frac{1-\upsilon^2}{R_{AFM}^{\frac{1}{2}}}\right)^{\frac{2}{3}} + \left[\frac{3\left(1-\upsilon^2\right)\left(F+6W\pi R_{SCP}+\sqrt{12W\pi R_{SCP}F_c\left(6W\pi R_{SCP}\right)^2}\right)}{4E\cdot R_{SCP}^{\frac{1}{2}}}\right]^{\frac{2}{3}} - \left[\frac{9W\pi\left(1-\upsilon^2\right)}{E}\right]^{\frac{2}{3}}\cdot R_{SCP}^{\frac{1}{3}}$$

where E is the elastic modulus of the indented SCP, R_{SCP} its radius, υ the Poisson ratio of the SCP, W the SCP adhesion energy with the support surface and R_{AFM} the radius of the indenter. The Poisson ration was assumed to be 0.5 (volume conservation upon indentation). E and W were free fit parameters. The elastic moduli of FN SCPs were on the order of 66 kPa and their surface energy varied only marginally between 20 and 30 µJ/m^2 for the different fits. Below typical deformation (δ) –force (F) data (black) and fits (red) for FN SCPs are shown:

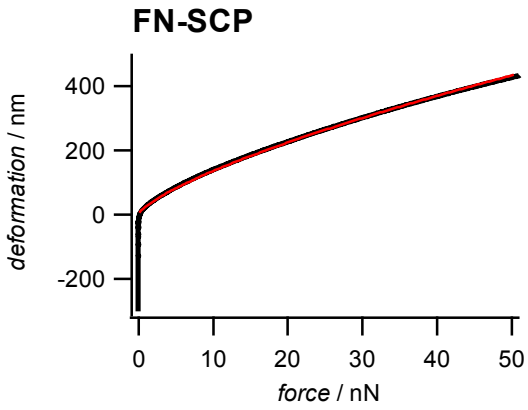

S6 Surface coating MA-copolymers

Materials

Ethanol, isopropanol, acetone and methyl ethyl ketone (MEK) were purchased from AppliChem GmbH. Hydrogen peroxide was purchased from Merck KGaA. Tetrahydrofuran (THF) and ammonia were purchased from Grüssing GmbH. (3-Aminopropyl)triethoxysilane (APTES) was purchased from Alfa Aesar. Maleic anhydride copolymers were purchased from Sigma Aldrich or a gift from the IPF Dresden.

Surface preparation

The coverslips were precleaned in an ultrasonic bath with MilliQ water for 30 min. After washing 3 times with MilliQ water they were cleaned a second time in an ultrasonic bath with 100% ethanol for another 30 min. The slides were washed 3 times in MilliQ water. For the removal of organic remnants and small particles a Radio Corporation of America (RCA) cleaning method was applied with a solution consisting of hydrogen peroxide, ammonia and MilliQ water in a ratio 1:1:5 for 10 min at 70°C. The cleaned slides were washed 2 times in MilliQ water and dried with nitrogen. For the covalent binding of the polymers, amines were established by amino silanization of the slides for 2 hrs with 20 mM APTES in an isopropanol/ MilliQ water solution in the ratio 9:1. Afterwards the slides were washed thoroughly with isopropanol and dried with nitrogen. After heating the slides for 1hrs at 120°C the polymers were spincoated at 4000 rpm for 30 sec onto the slides. Therefore filtrated (0.2 µm pore size) polymer solutions were prepared beforehand. Poly(octadecene-alt-maleic anhydride) (POMA; M_W 50000 g/mol) and poly(styrene-alt-maleic anhydride) (PSMA; M_W 20000 g/mol) were prepared in THF at a concentration of 0.16 wt% and 0.14 wt%, respectively. Poly(ethylene-alt-maleic anhydride) (PEMA; M_W 125000 g/mol) was prepared in a solution consistent of acetone and THF in the ratio 1:2 at a concentration of 0,3 wt%. Poly(propene-alt-maleic anhydride) (PPMA; M_W 39000 g/mol) was prepared in MEK at a concentration of 0.2 wt%. The slides were heated for 2 h at 120°C and afterwards washed with acetone to remove the redundant polymer.

S7 Stress and force distribution in contact zone

The JKR theory predicts that the pressure distribution underneath the SCP is governed by the interplay between elastic compression of the soft hydrogel matrix and adhesion between the FN and polymer surfaces.[3] Analytically, the pressure profile underneath the SCP can be described by:

$$p(r) = p_0\left(1-\frac{r^2}{a^2}\right) + p_1\left(1-\frac{r^2}{a^2}\right)^{-1/2}$$

$$p_0 = \frac{3E_{eff}}{2\pi R}, p_1 = \sqrt{\frac{3E_{eff}W}{2\pi a}}$$

where a is the contact radius, R is the radius of curvature (radius of SCPs), $E_{eff}=[4E/3(1-\nu^2)]$ is the effective elastic modulus, with ν the Poisson ratio and E the Young's modulus of the SCP, W is the work of adhesion, and r is the radial position from the center of the contact zone. Upon

adhesion the SCP elastically deform leading to positive contribution to the pressure, i.e. compressive stress (first part of *p(r)*), close to the center of the contact zone. At the edge of the contact area, adhesive contributions dominate, resulting in a region with negative pressure (second part of *p(r)*), see Figure S7a below.

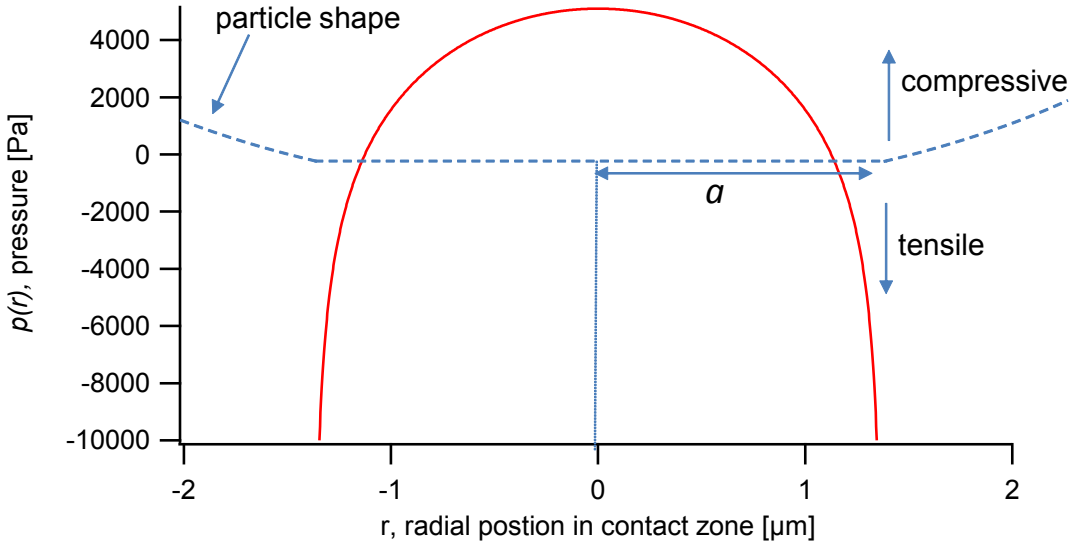

Figure S7a. The distribution of stress (red line) in the contact area on a POMA surface for $W = 160$ µJ/m^2 (POMA), $R = 10$ µm, $v = 0.5$, $E = 66$ kPa, $a = 1.38$ µm. When surfaces are maintained in contact by adhesion forces the stresses between the surfaces are tensile (second part of *p(r)*) at the edge of the contact and remain compressive (first part of *p(r)*) in the center of contact.

As can be seen from the equation above the pressure distribution *p(r)* depends on the radius of the SCPs (*R*) due to the. Generally, smaller SCPs lead to larger compressive stresses near the center of the contact zone, whereas the asymptotically increase of the tensile stress at the rim is largely independent of *R* (Figure S7b). Smaller SCPs ($R = 10$ µm dashed line) generate higher compressive forces acting on the FN layer as compared to larger SCPs ($R = 30$ µm solid line). However the difference between in the size range of SCP used here (10 µm and 30 µm) is rather small. Therefore the overall adhesion energies remained unchanged.

In addition, from the pressure distributions *p(r)* the force exerted on the individual FN molecules can be estimated (assuming an effective area of the FN molecules of 5.3×10^{-16} µm^2), see Figure S7b. The forces at the rim of the contact zone should represent a quantitative measure for the adhesion strength of FN to the polymer surfaces. Interestingly the range of high tensile forces >3

pN for at the rim of the contact zone roughly corresponds to the estimated desorption force of FN (on POMA) from cell studies.[4]

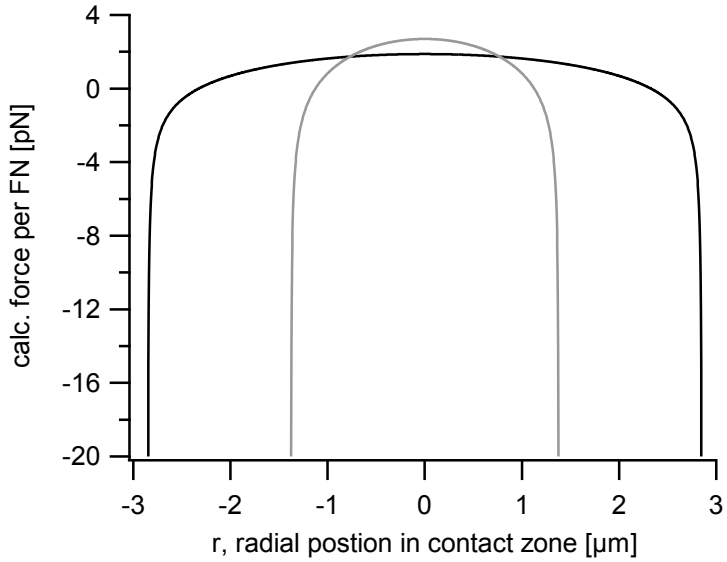

Figure S7b. Force per FN molecule distribution in the contact area for W = 160 µJ/m^2 (POMA value), E = 66kPa, ν = 0.5, *R* = 10 µm, a = 1.38 µm (dashed line), R = 30 µm, a = 2.85 µm (solid line).

S8 Reflection Interference Contrast Microscopy (RICM) measurements

Setup

RICM on an inverted microscope (Olympus IX73) was used to obtain the contact area between the microparticles and a hard glass surface. For illumination a monochromatic (530 nm) collimated LED (Thorlabs, Germany, M530L2-C1) was used. An Olympus 60 x NA 1.35 oil-immersion objective (UPLSAPO60XO/1,35 U Plan S Apo), additional polarizers and a quarter waveplate (Thorlabs, germany) to avoid internal reflections and a monochrome CMOS camera (UI-3360CP-M-GL, IDS Germany) were used to image the RICM patterns. To conduct the JKR measurements, both the contact radius (in RICM mode) and the particle radius (in transmission mode) were measured. Image acquisition was done using µManager (v1.4.16), data analysis was done using the image analysis software Image-J (v1.48) and the mathematical software IgorPro (v6.38, Wavemetrics, USA).

Determination of the contact radius

RICM was used to measure the contact radius formed by the SCPs resting on the polymer surface (Figure S8a). Polarized light waves reflected from the upper glass surface (I_1) and the surface of the bead (I_2) interact to create an interference image. The intensity at a given position in the image depends on the separation $h(x)$ between the two surfaces: $I(x) = I_1 + I_2 + 2 \cdot \mathrm{sqrt}(I_1 \cdot I_2) \cos[2k \cdot h(x) + \pi]$, where $k = 2\pi n/\lambda$, and n and λ are the index of refraction of water and the wavelength of the monochromatic light, respectively. In order to detect the interference pattern, stray light was reduced by an 'antiflex' technique. This is accomplished by crossed polarizer and analyzer filter with a λ/4-plate placed between the objective lens and the analyzer.[5]

Practical note: Although it is generally recommended to use the antiflex optics with polarization methods to avoid stray light generated in the microscope, we observed only little improvement in image contrast when using the antiflex setup. RICM images could be readily taken without polarizer, analyzer and quarter wave plate. This is possibly due to the rigorous use of antireflective lenses in the microscope and Thorlabs components.

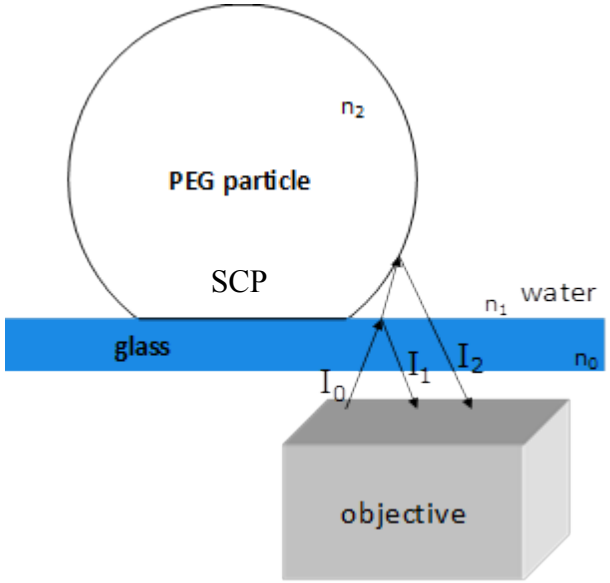

Figure S8a: Schematic drawing of the RICM principle.

Correction Factors

For analysis of the intensity distribution correction factors must be determined for finite aperture and geometry effects. To obtain the correction factors, we imaged hard, non-deformable glass beads on a glass surface in RICM mode (Figure S8b) with a known size. We recorded 5 glass beads with a diameter in the range of 10-20 µm and extracted the intensity profile. Using the

profiles, we reconstructed the shape of the beads and compared it to the known spherical shapes of the glass beads (glass bead radius R measured by light microscope), and determined the correction factors, see Pussak et al.[6]

Contact radius determination

To determine the contact radius a of the SCP on the polymer surface we reconstructed the height profile of the particles from the RICM images (see Figure S8c). This was done by determining the lateral $x(i)$ positions of the i-th minima and maxima by a self-written IgorPro procedure (Wavemetrics, USA). Next, the vertical position $y(i)$ of the maxima and minima were determined by

$$y(i) = \frac{i\lambda}{4n} + c_i ,$$

where n is the refractive index and λ the wavelength. The height profile was then reconstructed by plotting $y(i)$ vs $x(i)$ and fitting the data by a circle equation representing the assumed shape of the SCP:

$$y(x) = y_0 + \sqrt{R^2 - x^2} .$$

where R is the independently measured SCP radius and y_0 the vertical shift of the SCP center due to flattening of the SCP upon adhesion. The fit with y_0 as the only free fit parameter intersects with the x-axis and gives the contact radius a.

Figure S8c Left: schematic representation of the measurement setup. Bottom right: actual intensity profile of an adherent SCP showing 5 minima and 5 maxima. Top right: reconstructed surface profile of the SCP and the contact radius a at the intersection of the profile at $y = 0$.

Supporting Information References

1. J. Pelta, H. Berry, G. C. Fadda, E. Pauthe and D. Lairez, *Biochemistry*, 2000, 39, 5146-5154.
2. M. Glaubitz, N. Medvedev, D. Pussak, L. Hartmann, s. schmidt, C. A. Helm and M. Delcea, *Soft Matter*, 2014, DOI: 10.1039/c4sm00788c.
3. K. L. Johnson, K. Kendall and A. D. Roberts, *Proceedings of the Royal Society of London. A. Mathematical and Physical Sciences*, 1971, 324, 301-313.
4. T. Pompe, K. Keller, C. Mitdank and C. Werner, *European Biophysics Journal with Biophysics Letters*, 2005, 34, 1049-1056.
5. L. Limozin and K. Sengupta, *ChemPhysChem*, 2009, 10, 2752-2768.
6. D. Pussak, D. Ponader, S. Mosca, S. V. Ruiz, L. Hartmann and S. Schmidt, *Angewandte Chemie International Edition*, 2013, 52, 6084-6087.